ACS APPLIED MATERIALS & INTERFACES

Research Article

www.acsami.org

Thickness and Post-annealing Effects of the Sputtered La-Capping Layer Inserted between the TiN Gate and Hf-Based Dielectrics

Woo-Hee Kim,*,† Nae-In Lee, Jong-Ho Lee, and Kug-Hwan Kim*

Process Development Team, System LSI Division, Samsung Electronics, San #24 Nongseo-dong, Giheung-gu, Yongin, Gyeonggi-do 446-711, Korea

Supporting Information

ABSTRACT: We investigated effects of the sputtered La-capping layer inserted between TiN and Hf-based dielectrics, HfO_2 and $HfSiO_4/HfO_2$, mainly focusing on effective work function (EWF) and equivalent oxide thickness (EOT) changes by modulation of its thickness and post-metal annealing (PMA). The use of thin La capping up to 5 Å showed a linear flatband voltage (V_{FB}) shift of −60 mV/Å, regardless of gate dielectrics. However, with the increase of the La thickness, a slight increase in EOT was observed for HfO_2, whereas a negligible change in EOT was shown for the $HfSiO_4/HfO_2$ bilayer. It might be ascribed to the facile La oxidation, which acts as an additional oxide layer on both of the gate dielectrics. Meanwhile, high-temperature PMA exhibited slight reduction in V_{FB} as well as an EOT increase for both of the Hf-based dielectrics. On the basis of X-ray photoelectron spectroscopy (XPS) results, the reason for the slightly decreased EWF resulted from two competing dipoles formed by movements of oxygen vacancies (V_O) and La atoms during the PMA. Additionally, oxygen affinity and diffusion of the La-capping layer on both of the gate dielectrics are further discussed in conjunction with thermodynamic analyses, and thereby, schematic energy band diagrams were proposed by taking into account competing dipole layers by V_O movement and La diffusion.

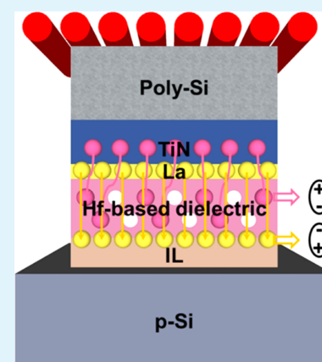

KEYWORDS: *Hf-based gate dielectrics, La-capping layer, thin films, effective work function, high κ, MOS capacitors*

1. INTRODUCTION

Because complementary metal-oxide-semiconductor field effect transistors (MOSFETs) are aggressively scaled down to a deep sub-micrometer regime for technology node beyond 45 nm, high-κ dielectrics in conjunction with metal gates should be introduced to meet the technology demands toward high device performance and low power consumption. Among several high-κ dielectric materials, the outstanding properties of Hf-based oxides have received a great deal of attention, mainly because of their high dielectric constant (∼25), large band gap (∼5.8 eV), and conduction band offset (∼1.4 eV), with good thermal stability in direct contact with the silicon channel.[1−6] However, the development of metal gates with work function near the Si band edges has been difficult in the case of Hf-based dielectrics. This might be attributed to several possible factors, including Fermi level pinning (FLP) and interfacial dipole formation.[7−9] Accordingly, it is the essential requirement that work function of the metal gate should be tailored by engineering the metal/dielectric interface.

To date, several research groups have reported the use of thin La-based capping layers between metal gates and Hf-based dielectric layers to controllably modulate the effective work function (EWF), especially for achievement of n-type metal gate performance.[9−11] Although the exact mechanism for shifting the EWF is still not clearly understood, the most compelling explanation may be attributed to interface dipoles formed at the high-κ/SiO_2 interfacial layer (IL).[11,12] Up to now, some plausible models have been proposed to explain the interfacial dipole formed in high-κ stacks, such as the FLP model, oxygen vacancy (V_O) model, Pauling electronegativity (EN) model, and oxygen areal density model.[11,13,14] Among them, Pauling EN and oxygen area density models are successful in explaining both of the effective dipole directions at the high-κ/SiO_2 interface induced by La- and Al-based capping materials employed for both n- and p-type MOSFETs, respectively.[5,11,13] Namely, according to their dipole models, it suggests that capping materials and oxygen behavior near the interface will play a significant role for the formation of interfacial dipoles. Nevertheless, it still requires more detailed investigation because the dipole formation is a complicated process not limited to only one model in some cases. Hence, it prompts us to comprehensively study the multiple micro-origins of the interfacial dipoles by inserted capping layer effects to extend more degree of freedom in fabricating high-performance MOSFET devices considering real integration schemes.

In this report, effects of the La-capping layer inserted between the TiN gate and two kinds of Hf-based gate dielectrics, which are HfO_2 and $HfSiO_4/HfO_2$, dependent upon its thickness and post-high-temperature annealing, were systematically investigated, mainly focusing on changes in EWF and equivalent oxide thickness (EOT). Here, TiN is the

Received: January 23, 2014
Accepted: March 18, 2014
Published: March 18, 2014

 © 2014 American Chemical Society

essential requirement as a gate material because it has been practically implemented together with Hf-based dielectrics beyond 45 nm technology regime for industry. In conjunction with Hf-based oxides, the La-induced flatband voltage (V_{FB}) shift is the top choice as well for tuning the EWF of midgap metals to the Si conduction band edge for n-type MOSFETs. Accordingly, the electrical properties of ΔEOT and ΔEWF were evaluated in TiN/La/Hf-based dielectrics/p-type Si MOS structures. Additionally, La oxygen affinity and its diffusion as well as V_O movements throughout the gate stacks were further discussed, taking into account their chemical binding structures and thermodynamic behavior in terms of standard Gibbs free energy change, and thereby, we clearly revealed dipole behavior by the oxygen vacancies and La diffusion model.

2. EXPERIMENTAL SECTION

2.1. Capacitor Fabrication. MOS capacitors were fabricated on p-type Si substrate cleaned in a diluted HF dip and a deionized water rinse. After the wet cleaning, 10 Å thick SiO_2 IL was chemically grown on the Si substrate, subsequently followed by gate dielectric deposition. Here, two kinds of dielectric layers were employed: one is 18 Å thick HfO_2, and the other is a stacked bilayer composed of $HfSiO_4/HfO_2$ with 4 and 14 Å, where $HfSiO_4$ (Hf/Si = 1:1) and HfO_2 were prepared by metallorganic chemical vapor deposition (MOCVD) with tetrakis(tertiarybutoxy)hafnium (HTB) and tetraethylorthosilicate (TEOS) and atomic layer deposition (ALD) with hafnium tetrachloride ($HfCl_4$), respectively. Then, 1−5 Å thick La-capping layers were deposited by DC/RF magnetron sputtering at 20 mTorr with plasma power of 50 W. Subsequently, a 20 Å thick TiN gate electrode was formed by DC/RF reactive magnetron sputtering at 20 mTorr with plasma power of 500 and 2000 W, respectively, and 100 Å thick poly-Si deposition by CVD was performed with SiH_4 and PH_3 to not only suppress the TiN oxidation but also provide significant oxide regrowth of the high-κ/SiO_2 IL region from external oxygen ingress during the post-annealing process. It is noted that all of the prepared samples were subjected to post-metal annealing (PMA) at 1000 °C using spike rapid thermal annealing, except for w/o PMA samples. Finally, all of the gate stacks were patterned to define the gate area by photolithography and dry etching.

2.2. Characterizations. The thickness of the thin films was measured by in-line X-ray photoelectron spectroscopy (XPS) and a spectroscopic ellipsometer, which were elaborately calibrated using high-resolution transmission electron microscopy (TEM). The chemical composition and binding structures were analyzed by XPS. Capacitance−voltage (*C*−*V*) measurements were experimentally analyzed in parallel mode at 100 kHz with a gate area of 100 × 100 μm^2 using a precision semiconductor parameter analyzer (Agilent B1500). For all of the capacitor samples, the amount of *C*−*V* hysteresis obtained by sweeping the measurement voltage from accumulation to inversion and back again was found to be negligible below ~20 mV. From the *C*−*V* data, the North Carolina State University (NCSU) CVC analysis program was invoked to elaborately extract the device parameters, such as V_{FB}, EWF, and EOT. The leakage current density−voltage (*J*−*V*) characteristics were evaluated by the same Agilent equipment. All of the electrical tests were carefully carried out in a dark probe station. All of the characterization equipment were interfaced with a computer, and a switch matrix was used for automated testing. Besides, the standard Gibbs free energy changes are considered in terms of the standard enthalpy and entropy of the reaction, using $\Delta G° = \Delta H° - T\Delta S°$. Analytic methods introduced for the M−X (M = La, Hf, and Si, and X = O) system were applied to study oxygen affinity of the metals.[15,16]

3. RESULTS AND DISCUSSION

La thickness dependence upon EWF and EOT shifts were evaluated in TiN/La/Hf-based dielectrics/p-type Si MOS structures. Figure 1 shows the experimentally measured and

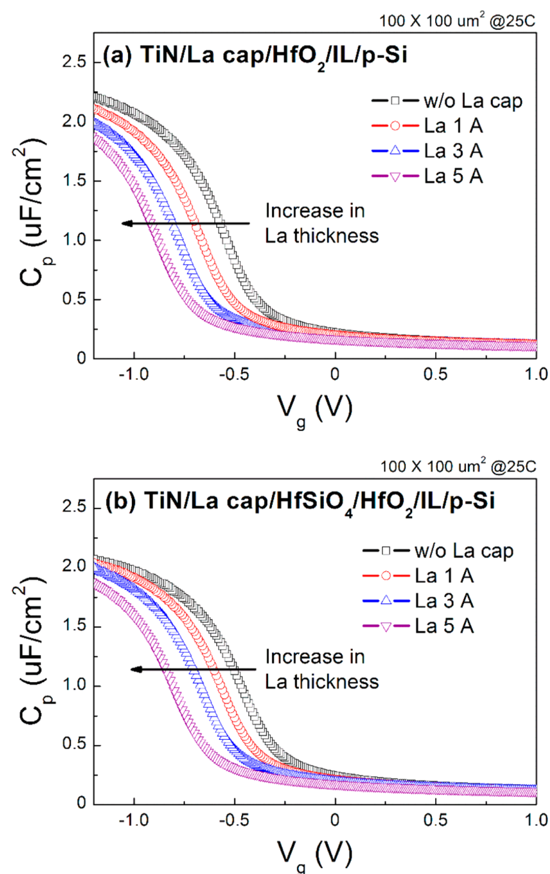

Figure 1. Measured and CVC-fitted *C*−*V* curves of the TiN/La/Hf-based dielectrics/IL/p-type Si MOS capacitor as a function of La thickness: (a) HfO_2 and (b) $HfSiO_4/HfO_2$.

CVC-fitted *C*−*V* curves of the MOS capacitors, indicating the dependence of La thickness (w/o La, 1, 3, and 5 Å) on HfO_2 and bilayer $HfSiO_4/HfO_2$ gate dielectrics. The distinctive shift in flatband voltage to the negative direction was observed with increasing the La thickness, regardless of the gate dielectrics. Nevertheless, there is no stretch or distortion in all of the *C*−*V* curves, which suggests that movement of bulk charges might seem to be attributed to the flatband voltage shift rather than interface trap charges.[8,9]

Figure 2 shows the CVC-extracted EWF and EOT plots as a function of La thickness. For both of the dielectric cases, as the La thickness increased up to 5 Å, EWF values decreased with −60 mV/Å slope. According to the previous reports from several research groups, the origin in the EWF shift has been regarded as the dipole layer formation related to La atoms diffused to high-κ/SiO_2 IL through the oxide layer during deposition and post-annealing process.[8,11] Accordingly, the interface dipole strength by La diffusion has a strong relationship with the incorporated La concentration. The relation between the EWF shift and La concentration in the formed dipole layer is as follows:[12]

$$|\overrightarrow{P_{La}}| = |q\vec{d}| = \left|\frac{\Delta \mathrm{EWF}\varepsilon_{dipole}}{\Delta N_{La}}\right| \quad (1)$$

where P_{La} is the dipole moment per 1 La atom, ΔN_{La} is the change of the area density of the incorporated La atoms in the dipole layer, ΔEWF is the EWF change with respect to that of pure HfO_2 and $HfSiO_4/HfO_2$, and ε_{dipole} is a permittivity of the

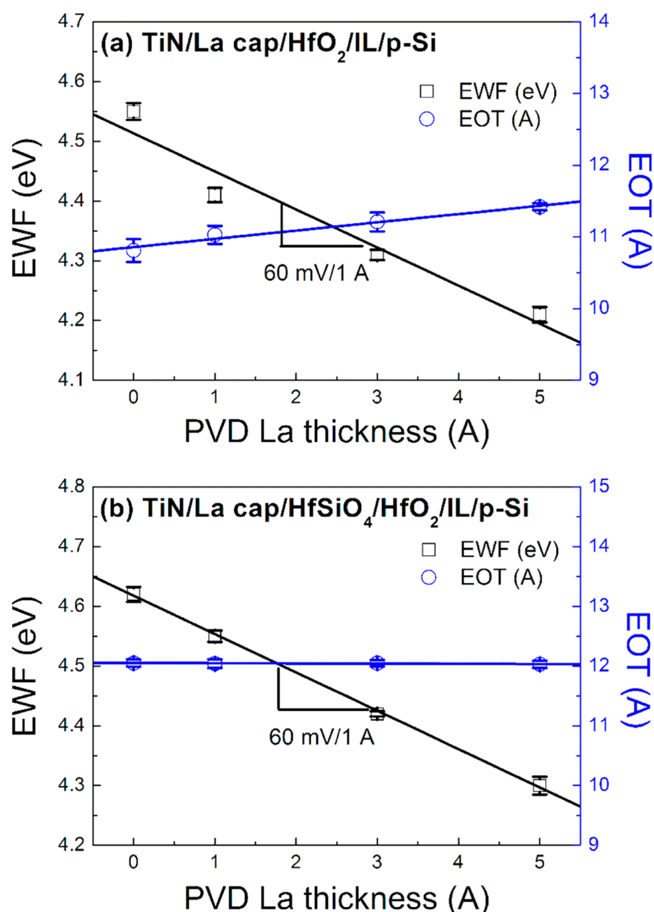

Figure 2. CVC-extracted EWF and EOT plots of the TiN/La/Hf-based dielectrics/IL/p-type Si MOS capacitor as a function of La thickness: (a) HfO_2 and (b) $HfSiO_4/HfO_2$.

dipole layer. The ε_{dipole} values indicated herein should be almost the same for all of the samples. Accordingly, it is found that ΔEWF is linearly proportional to ΔN_{La}, dependent upon La thickness, agreeing well with the current results. According to the increasing La thickness on HfO_2 gate dielectric, a slight increase in EOT was observed (10.8, 11.0, 11.2, and 11.4 Å), while a negligible change in EOT (~12.0 Å) was shown for that on $HfSiO_4/HfO_2$ bilayer dielectric. It is worth noting that La is prone to be easily oxidized by taking up the oxygen from HfO_2 and $HfSiO_4$ as well as the IL region, leading to the formation of large amounts of oxygen vacancies (V_O). Thereby, it acts as one of the series oxide layers contributing to the EOT change. Namely, when taking into account the net dielectric constants for both of the dielectric cases, La_2O_3 on HfO_2 is likely to result in only oxide thickening without any increment of the dielectric constant, whereas the increased dielectric constant and oxide thickness were expected for that on $HfSiO_4/HfO_2$. More discussion will be provided later in conjunction with thermodynamic analyses.

By introducing a limited-source diffusion equation, we further determine the detailed factors related to ΔN_{La} as follows:

$$N_{La}(x, t) = \frac{Q}{\sqrt{\pi D t}} e^{(-x^2/4Dt)} \quad (2)$$

where Q is the total amount of La atoms per unit area, D is the diffusion coefficient, x is the diffusion length, and t is the diffusion time. Given the Gaussian distribution, it can be inferred that the area density of the incorporated La atoms is synthetically correlated with diffusion length, time, and diffusivity depending upon the annealing temperature.

Accordingly, we investigated the PMA effect with the La-capping layer with a thickness of 3 Å. Figure 3 shows the experimentally measured and CVC-fitted $C-V$ curves of the MOS capacitors indicating the PMA effects (w/o PMA and 1000 °C) on both the HfO_2 and stacked $HfSiO_4/HfO_2$ gate dielectrics. For both of the cases, the high-temperature PMA led to slight reduction in the maximum capacitance values mainly because of the oxide regrowth by oxygen ingress from the upper TiN layer, as we will discuss later. In addition, after the PMA, a slightly negative shift of V_{FB} was observed without any $C-V$ distortion as well. However, despite high-temperature annealing, there was no significantly noticeable V_{FB} shift, which is somehow different from what we were expecting from the diffusion equation above.

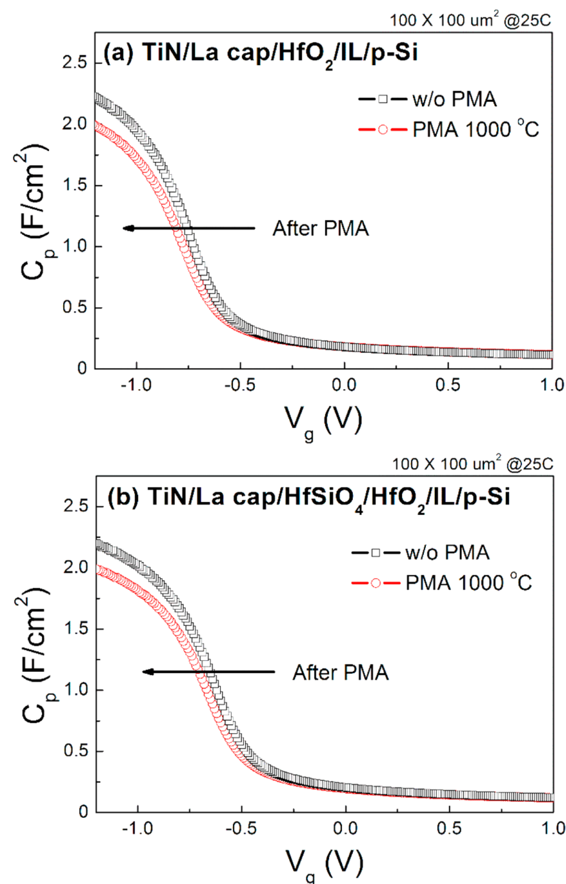

Figure 3. Measured and CVC-fitted $C-V$ curves of the TiN/La/Hf-based dielectrics/IL/p-type Si MOS capacitor before and after the PMA: (a) HfO_2 and (b) $HfSiO_4/HfO_2$.

To clarify the main cause for this, the CVC-extracted EWF and EOT values before and after PMA at 1000 °C were plotted in Figure 4. Although the high-temperature PMA results in slight EOT thickening, more uniform and lower EWF values are achieved, as compared to w/o PMA samples. In particular, it is noted that both of the samples without PMA exhibited a broad range of EWF shifts, suggesting partially random diffusion of La atoms through the intrinsic defect sites, such as V_O existing with several charged states in the thin Hf-based

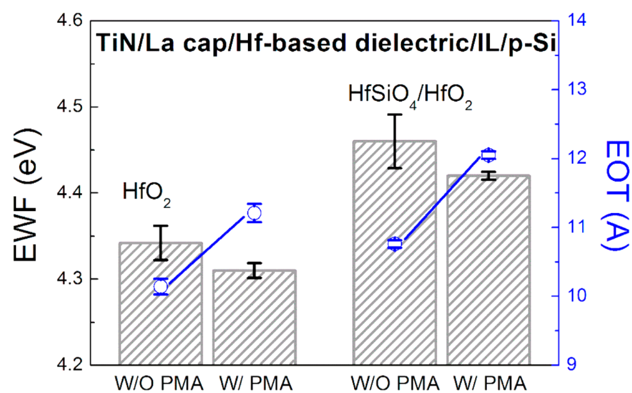

Figure 4. CVC-extracted EWF and EOT plots of the TiN/La/Hf-based dielectrics/IL/p-type Si MOS capacitor before and after the PMA.

dielectric layers, which presumably originated from the sputtered kinetic energy during the deposition.[17] However, as the samples undergo high-temperature annealing, they are subjected to the competing process by two major dipole factors, which are oxygen vacancies and La-induced interface dipoles, contributing to the negative V_{FB} shift. As described above, the increment of the V_O concentration in the Hf-based dielectrics is caused by oxygen movement to the La layer. Without the PMA, it mainly contributed to the low EWF values, forming a dipole layer by electron transfer from the V_O in Hf-based dielectrics to La as well as additional dipoles by partially diffused La atoms.[18,19] However, during the PMA, the V_O is partially passivated by a small amount of oxygen supplied from the upper TiN layer and simultaneously counterbalanced by La-induced dipoles.[11,20] With the increasing of the annealing temperature up to 1000 °C, the latter interface dipoles might have a more dominant role, resulting in a slight negative shift of EWF values.

Figure 5 shows angle-resolved XPS spectra of Hf 4f and La 3d before and after the PMA of HfO_2 dielectric samples with 5 Å thick La. After the high-temperature PMA, the Hf 4f doublet peak positions were shifted to a higher binding energy (Hf $4f_{7/2}$ = 17.8 and 18.1 eV, with a 1.4 eV interval, respectively), as shown in Figure 5a, suggesting the partial V_O passivation from oxygen inside the TiN layer during the annealing.[20,21] The reduction of the oxidized Ti component leading to IL regrowth upon high-temperature annealing was also observed elsewhere.[6] The XPS spectra in the $La_{5/2}$ binding energy region were composed of two broad peaks in Figure 5b. From the peak deconvolution, we note that the two kinds of chemical bonding structures made up of La−O at 835.2 and 839.4 eV and La−O−Si at 836.5 and 839.8 eV were observed for both of the cases.[11,22] The weak La−O−Si peaks with strong La−O bonding were clearly shown, even for the w/o PMA sample, indicating the partial La diffusion during the deposition. However, after the PMA, La−O−Si bonding became much more dominant, as compared to La−O bonding, because of the La diffusion during the high-temperature annealing, well agreeing with electrical results above.

Meanwhile, to further understand the oxygen affinity and La diffusion mechanism through both of the Hf-based oxides based on thermodynamic behavior, the standard Gibbs free energy change is considered in terms of the standard enthalpy and entropy of the reaction. Figure 6 plots the Gibbs free energy for the Si, Hf, and La systems as a function of the temperature. The

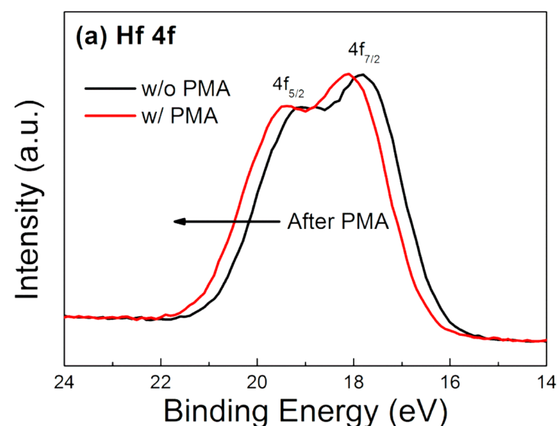

(a)

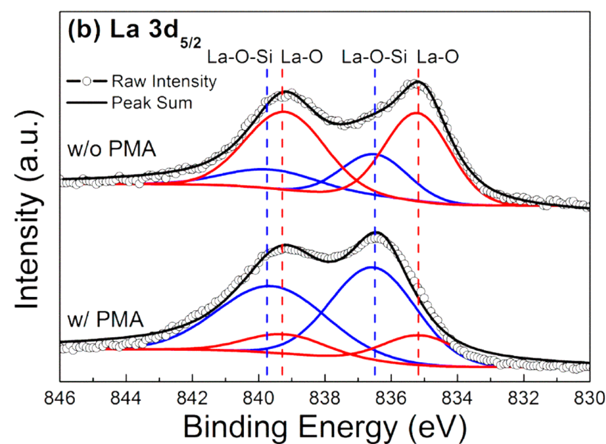

(b)

Figure 5. (a) Hf 4f and (b) La 3d XPS spectra before and after the PMA for the HfO_2 sample with 5 Å thick La.

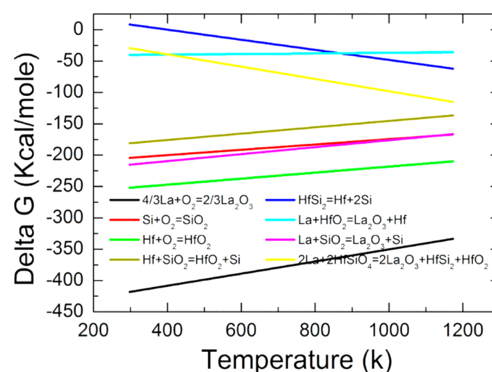

Figure 6. Standard Gibbs free energy plots for the Si, Hf, and La systems as a function of the temperature.

standard Gibbs free energy change for the formation of metal oxide can be expressed by the following equations:

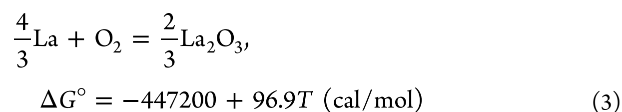

$$\frac{4}{3}\text{La} + \text{O}_2 = \frac{2}{3}\text{La}_2\text{O}_3,$$
$$\Delta G^\circ = -447200 + 96.9T \ (\text{cal/mol}) \quad (3)$$

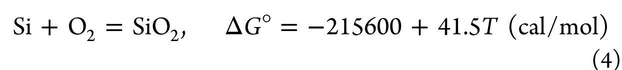

$$\text{Si} + \text{O}_2 = \text{SiO}_2, \quad \Delta G^\circ = -215600 + 41.5T \ (\text{cal/mol}) \quad (4)$$

dx.doi.org/10.1021/am500490u | ACS Appl. Mater. Interfaces 2014, 6, 5199−5205

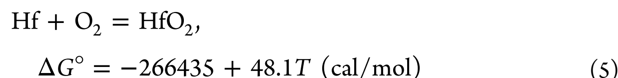

$$\mathrm{Hf + O_2 = HfO_2,} \quad \Delta G^\circ = -266435 + 48.1T \ \mathrm{(cal/mol)} \tag{5}$$

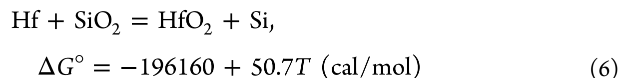

$$\mathrm{Hf + SiO_2 = HfO_2 + Si,} \quad \Delta G^\circ = -196160 + 50.7T \ \mathrm{(cal/mol)} \tag{6}$$

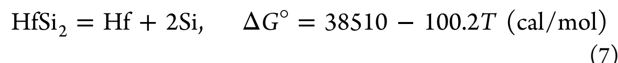

$$\mathrm{HfSi_2 = Hf + 2Si,} \quad \Delta G^\circ = 38510 - 100.2T \ \mathrm{(cal/mol)} \tag{7}$$

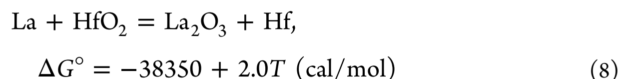

$$\mathrm{La + HfO_2 = La_2O_3 + Hf,} \quad \Delta G^\circ = -38350 + 2.0T \ \mathrm{(cal/mol)} \tag{8}$$

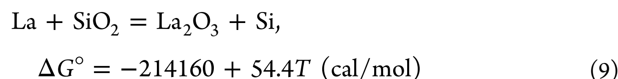

$$\mathrm{La + SiO_2 = La_2O_3 + Si,} \quad \Delta G^\circ = -214160 + 54.4T \ \mathrm{(cal/mol)} \tag{9}$$

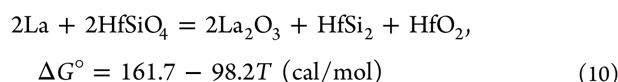

$$\mathrm{2La + 2HfSiO_4 = 2La_2O_3 + HfSi_2 + HfO_2,} \quad \Delta G^\circ = 161.7 - 98.2T \ \mathrm{(cal/mol)} \tag{10}$$

where ΔG° is the standard Gibbs free energy change of reaction and T is the absolute temperature. The plot of ΔG° against temperature mainly indicates the oxidation and dissociation behaviors when the reactions are considered in terms of the consumption of 1 mol of oxygen. At the onset of the La deposition on HfO_2 dielectric, it is more likely to be oxidized by scavenging the oxygen from the HfO_2 layer, leading to the additional V_O formation. In the case of the La deposition on the $HfSiO_4/HfO_2$ bilayer, it undergoes spontaneous oxidation as well. However, unlike the HfO_2 dielectric case, the formation of $HfSi_2$ seems to be also energetically favorable. It implies that the random diffusion of La atoms might be partially blocked during the deposition, leading to more EWF deviation than that on HfO_2 dielectric, which has good correspondence with the results shown in Figure 4 (4.34 ± 0.02 eV for HfO_2 and 4.46 ± 0.03 eV for $HfSiO_4/HfO_2$ w/o PMA). However, formed $HfSi_2$ tends to be dissociated spontaneously at high temperatures, and thereby, La diffusion through the $HfSiO_4/HfO_2$ bilayer might progress favorably during the PMA.

Figure 7 shows the Si, Hf, and La predominance phase diagram as a function of the oxygen and nitrogen partial pressures at a temperature of 1273 K. The equilibrium of O_2 or N_2 pressure can be derived from the standard Gibbs free energy change associated with the M−O or M−N system (M = La, Hf, and Si).

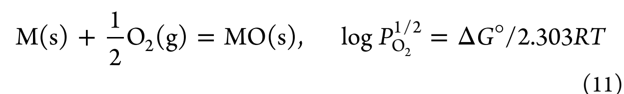

$$\mathrm{M(s)} + \frac{1}{2}\mathrm{O_2(g) = MO(s)}, \quad \log P_{O_2}^{1/2} = \Delta G^\circ/2.303RT \tag{11}$$

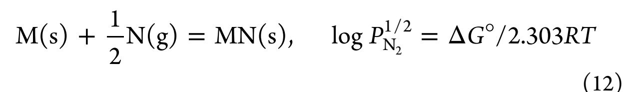

$$\mathrm{M(s)} + \frac{1}{2}\mathrm{N(g) = MN(s)}, \quad \log P_{N_2}^{1/2} = \Delta G^\circ/2.303RT \tag{12}$$

The partial pressure of oxygen in a system is commonly referred to as its oxygen potential, $\mu O_2 = \mu O_2^\circ + RT \ln P_{O_2}$, where R is the gas constant. Given the predominance phase diagram, the oxygen affinities in the oxidation reaction follow the order La > La_2O_3 > HfO_2 > SiO_2. In other words, the incorporation of oxygen from the HfO_2 and SiO_2 underlayers into La is energetically favorable, leading to more V_O formation inside the dielectric layers. In addition to dipole formation by the sputtered La diffusion, the V_O can play the key role of shifting the EWF to the negative direction, even without La-induced dipoles, by post-high-temperature annealing and also facilitate the La diffusion dielectric layer region during the PMA.

On the basis of the above discussion from thermodynamic consideration in conjunction with electrical and chemical analyses, Figure 8a schematically represents the oxygen

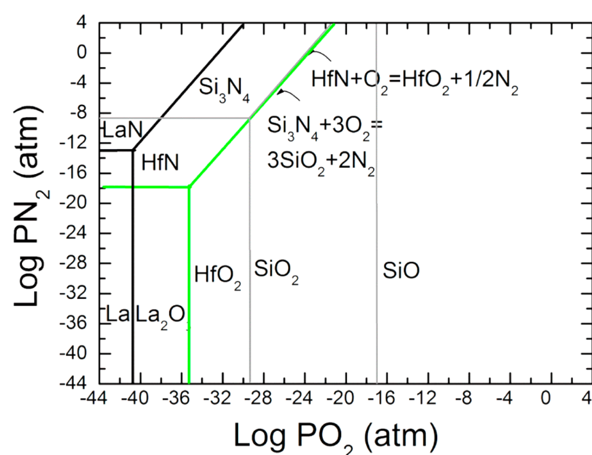

Figure 7. Si−Hf−Ti predominance phase diagram as a function of oxygen and nitrogen partial pressures at a temperature of 1273 K.

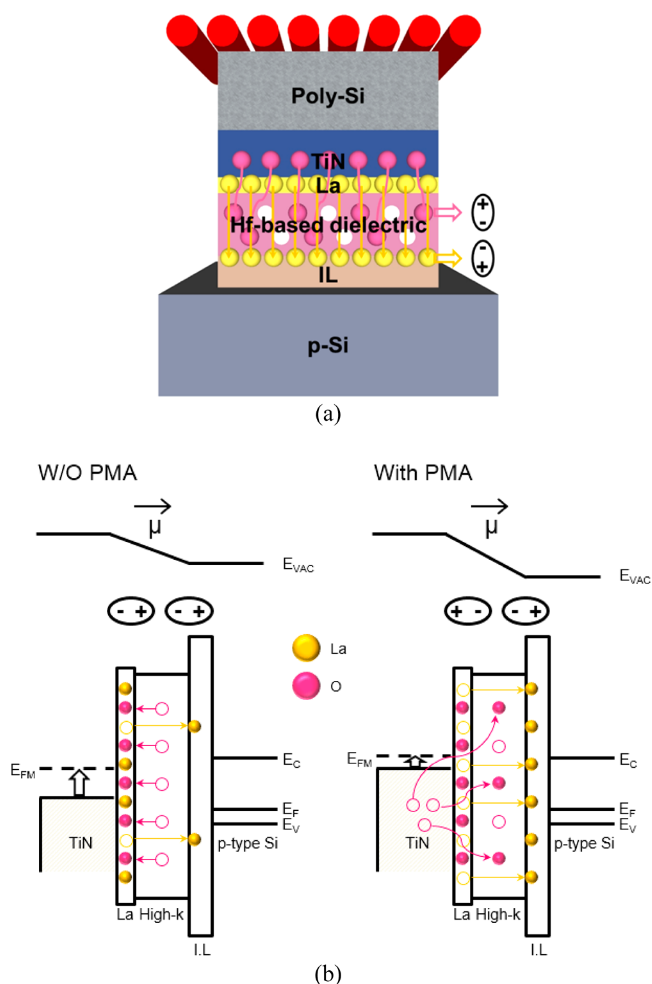

Figure 8. (a) Schamical illustration and (b) proposed energy band diagrams for the oxygen vacancies and La diffusion model.

dx.doi.org/10.1021/am500490u | ACS Appl. Mater. Interfaces 2014, 6, 5199−5205

vacancies and La diffusion model during the PMA process. Here, both the oxygen affinity and diffusion behavior of the La-capping layer are entirely described. For before and after the PMA, the proposed energy band diagrams are illustrated in Figure 8b. The as-deposited La film brings about additional oxygen vacancies from oxygen scavenging as well as partial diffusion of La atoms in the Hf-based dielectric layer, resulting in the initial dipole formation without the PMA. However, with the PMA, the V_O tends to partially turn back from the upper TiN layer, as opposed to the initial dipole direction. Nevertheless, additional dipoles by the diffused La atoms can compensate more than the opposed dipoles from oxygen movement, leading to more EWF lowering. Therefore, it implies that a comprehensive understanding related to oxygen affinity and diffusion of La is required to meet the EWF and EOT targets for successful implementation of the La-capping layer with respect to process integration.

4. CONCLUSION

In summary, the effects of the sputtered La-capping layer located between the TiN gate and two Hf-based dielectrics, HfO_2 and $HfSiO_4/HfO_2$, were extensively investigated, focusing the changes in EWF and EOT values by thickness and high-temperature PMA. For both of the dielectrics, it was found that linearly negative EWF shifts proportional to the La thickness increase up to 5 Å were observed. The slight EOT increment was accompanied by the increase in La thickness on HfO_2 samples, whereas that on $HfSiO_4/HfO_2$ samples was maintained, regardless of La thickness. It might be attributed to facile oxidation of La from Hf-based dielectrics and SiO_2 IL. The La is thermodynamically liable to be oxidized in terms of standard Gibbs free energy and oxygen affinity. Meanwhile, a slight reduction in EWF and an EOT increase were exhibited with the PMA for both dielectric cases. Although interface diploes induced by La diffusion become a more dominant factor than V_O passivation from upper TiN after the high-temperature PMA, it is worth noting that both of the competing processes during the deposition and PMA can contribute to the EWF shift. Therefore, it is envisaged that comprehensive studies based on electrical, chemical, and thermodynamic analyses enable the La-capping layer to be successfully implemented for process integration.

■ ASSOCIATED CONTENT

Supporting Information

(1) Leakage data of the TiN/La/Hf-based dielectrics/IL/p-type Si MOS capacitor, (2) formation of the La-induced interface dipole layer, (3) TEM−energy-dispersive spectrometry (EDS) data of the PMA La/HfO_2/IL/Si sample, and (4) EWF data of the TiN/La/Hf-based dielectrics/IL/p-type Si MOS capacitor. This material is available free of charge via the Internet at http://pubs.acs.org.

■ AUTHOR INFORMATION

Corresponding Authors

*E-mail: hanpos7@gmail.com.
*E-mail: kughwan.kim@gmail.com.

Present Address

†Woo-Hee Kim: Department of Chemical Engineering, Stanford University, 381 North South Mall, Stanford, California 94305, United States.

Notes

The authors declare no competing financial interest.

■ REFERENCES

(1) Wang, Y.; Wang, H.; Ye, C.; Zhang, J.; Wang, H.; Jiang, Y. Interfacial reaction and electrical properties of HfO_2 film gate dielectric prepared by pulsed laser deposition in nitrogen: Role of rapid thermal annealing and gate electrode. *ACS Appl. Mater. Interfaces* **2011**, *3*, 3813−3818.

(2) Ramana, C. V.; Noor-A-Alam, M.; Gengler, J. J.; Jones, J. G. Growth, structure, and thermal conductivity of yttria-stabilized hafnia thin films. *ACS Appl. Mater. Interfaces* **2012**, *4*, 200−204.

(3) Mahata, C.; Byun, Y.-C.; An, C.-H.; Choi, S.; An, Y.; Kim, H. Comparative study of atomic-layer-deposited stacked (HfO_2/Al_2O_3) and nanolaminated ($HfAlO_x$) dielectrics on $In_{0.53}Ga_{0.47}A$. *ACS Appl. Mater. Interfaces* **2013**, *5*, 4195−4201.

(4) Kim, H. K.; Yu, I.-H.; Lee, J. H.; Hwang, C. S. Interfacial dead-layer effects in Hf-silicate films with Pt or RuO_2 gates. *ACS Appl. Mater. Interfaces* **2013**, *5*, 6769−6772.

(5) Wilk, G. D.; Wallace, R. M.; Anthony, J. M. High-κ gate dielectrics: Current status and materials properties considerations. *J. Appl. Phys.* **2001**, *89*, 5243−5275.

(6) Maeng, W. J.; Kim, W.-H.; Koo, J. H.; Lim, S. J.; Lee, C.-S.; Lee, T.; Kim, H. Flatband voltage control in p-metal gate metal-oxide-semiconductor field effect transistor by insertion of TiO_2 layer. *Appl. Phys. Lett.* **2010**, *96*, 082905.

(7) Wang, X. P.; Yu, H. Y.; Li, M. F.; Zhu, C. X.; Biesemans, S.; Chin, A.; Sun, Y. Y.; Feng, Y. P.; Lim, A.; Yeo, Y.-C.; Loh, W. Y.; Lo, G. Q.; Kwong, D.-L. Wide V_{fb} and V_{th} tunability for metal-gated MOS devices with HfLaO gate dielectrics. *IEEE Electron Device Lett.* **2007**, *28*, 258−260.

(8) Chiang, C. K.; Wu, C. H.; Liu, C. C.; Lin, J. F.; Yang, C. L.; Wu, J. Y.; Wang, S. J. Effects of La_2O_3 capping layers prepared by different ALD lanthanum precursors on flatband voltage tuning and EOT scaling in $TiN/HfO_2/SiO_2/Si$ MOS structures. *J. Electrochem. Soc.* **2011**, *158*, H447−H451.

(9) Alshareef, H. N.; Quevedo-Lopez, M.; Wen, H. C.; Harris, R.; Kirsch, P.; Majhi, P.; Lee, B. H.; Jammy, R. Work function engineering using lanthanum oxide interfacial layers. *Appl. Phys. Lett.* **2006**, *89*, 232103.

(10) Guha, S.; Paruchuri, V. K.; Copel, M.; Narayanan, V.; Wang, Y. Y.; Batson, P. E.; Bojarczuk, N. A.; Linder, B.; Doris, B. Examination of flatband and threshold voltage tuning of HfO_2/TiN field effect transistors by dielectric cap layers. *Appl. Phys. Lett.* **2007**, *90*, 092902.

(11) Maeng, W. J.; Kim, W.-H.; Kim, H. Flat band voltage (V_{FB}) modulation by controlling compositional depth profile in La_2O_3/HfO_2 nanolaminate gate oxide. *J. Appl. Phys.* **2010**, *107*, 074109.

(12) Yamamoto, Y.; Kita, K.; Kyuno, K.; Toriumi, A. Study of La-induced flat band voltage shift in metal/$HfLaO_x/SiO_2$/Si capacitors. *Jpn. J. Appl. Phys.* **2007**, *46*, 7251−7255.

(13) Kita, K.; Toriumi, A. Origin of electric dipoles formed at high-k/SiO_2 interface. *Appl. Phys. Lett.* **2009**, *94*, 132902.

(14) He, G.; Zhu, L.; Sun, Z.; Wan, Q.; Zhang, L. Integrations and challenges of novel high-*k* gate stacks in advanced CMOS technology. *Prog. Mater. Sci.* **2011**, *56*, 475−572.

(15) Samsonov, G. V.; Vinitski, I. M. *Handbook of Refractory Compounds*; IFI/Plenum: New York, 1980; pp 20−25.

(16) Chang, H. L.; Liang, M. S. Oxygen vacancy estimation of high k metal gate using thermal dynamic model. *Appl. Phys. Lett.* **2010**, *97*, 041912.

(17) Foster, A.; Gejo, F. L.; Shluger, A.; Nieminen, R. Vacancy and interstitial defects in hafnia. *Phys. Rev. B: Condens. Matter Mater. Phys.* **2002**, *65*, 174117.

(18) Guha, S.; Narayanan, V. Oxygen vacancies in high dielectric constant oxide-semiconductor films. *Phys. Rev. Lett.* **2007**, *98*, 196101.

(19) Cartier, E. The role of oxygen in the development of Hf-base high-k/metal gate stacks for CMOS technologies. *ECS Trans.* **2010**, *33*, 83−94.

(20) Frank, M. M.; Marchiori, M.; Bruley, J.; Fompeyrine, J.; Narayanan, V. Epitaxial strontium oxide layers on silicon for gate-first and gate-last TiN/HfO_2 gate stack scaling. *Microelectron. Eng.* **2011**, *88*, 1312−1316.
(21) Lee, P. H.; Dai, J. Y.; Chan, H. L. W.; Choy, C. L. Two-step interfacial reaction of HfO_2 high-*k* gate dielectric thin films on Si. *Ceram. Int.* **2004**, *30*, 1267−1270.
(22) Cople, M.; Cartier, E.; Ross, F. M. Formation of a stratified lanthanum silicate dielectric by reaction with Si(001). *Appl. Phys. Lett.* **2001**, *78*, 1607−1609.